SAE TECHNICAL PAPER SERIES

930226

Active Human Surrogate Control of a Motorcycle: Stabilizing and De-Stabilizing

Shawn P. McGuan
Mechanical Dynamics, Inc.

The Engineering Society For Advancing Mobility Land Sea Air and Space®
INTERNATIONAL

International Congress and Exposition
Detroit, Michigan
March 1-5, 1993

400 Commonwealth Drive, Warrendale, PA 15096-0001 U.S.A. Tel: (412)776-4841 Fax:(412)776-5760

ISSN 0148-7191

Printed in USA

930226

Active Human Surrogate Control of a Motorcycle: Stabilizing and De-Stabilizing

Shawn P. McGuan
Mechanical Dynamics, Inc.

ABSTRACT

Two aspects of a motorcycle injury crash are studied in this paper. 1) What were the rider's actions which led to unsafe handling of the motorcycle? 2) What were the injury-producing mechanisms present during the crash? This inquiry illustrates methods and procedures which are useful for motorcycle safety design as well as reliability analysis. The ADAMS™ mechanical system simulation program is used to generate computer models of a motorcycle and rider under rider control to simulate a mild lane change maneuver. Manual control and vehicle response characteristics are evaluated for a cases involving a system disturbance such as an encounter with a road pothole during the turning phase in the lane change. For the case when the rider/cycle system becomes unstable resulting in a crash, the 3-dimensional joint strength model for the human surrogate rider model switches from an active, motorcycle control model (pre-crash phase) to a passive, rebound model (crash phase), derived from the Hybrid III crash dummy. A biomechanical stress review is then performed to study the injury potential resulting from the crash.

INTRODUCTION

MANUAL CONTROL OF MOTORCYCLES has long been of practical and theoretical interest. Since motorcycles, or single-track vehicles in general, can be susceptible to environmental disturbances and require constant rider attention, they present unique problems in stability and control.

In the early seventies, Sharp [1-3] developed equations of motion and a simulation model for the motorcycle vehicle. Weir [4-6] applied systems theory and manual control to the stability and control of the rider/cycle system. This work has extended by Eaton [7], Rice [8], Weir [9] and others.

This paper begins with a discussion of the 3-dimensional, non-linear computer models of the motorcycle and the human surrogate rider used in this inquiry. The mass ratio of the rider to motorcycle is high enough that the multiple-loop, parallel compensator presented in Weir [6], for path regulation and capsize stability is implemented. Three simulation cases are then presented for the lane-change maneuver. The first case presents the steady-state maneuver, stabilized and guided using rider control with proper rider neuro-muscular actuation lags. For the second case, a disturbance is introduced with the motorcycle encountering a pothole and the rider compensating during the turn. In this case, "anticipation" of the obstacle is included in the rider model by tightening the actuation response lags. For the final case, rider anticipation is not included contributing to capsize instability and a crash.

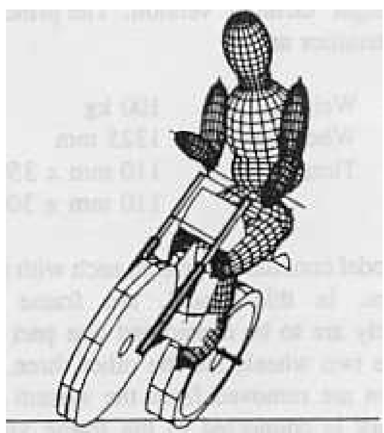

Fig. 1 The Rider-Controlled Lane Change Maneuver.

MODEL DESCRIPTIONS

THE MOTORCYCLE MODEL - The motorcycle dynamics comprise the controlled element of the rider/cycle system. These dynamics can be characterized analytically via a system of differential equations. Of necessity, these differential equations were originally of linear form, Weir [4], or a reduced degree-of-freedom set of non-linear equations, Roland [10].

With the evolution of software tools such as ADAMS [11], it is now convenient to generate a system of non-linear (differential/algebraic) equations representing a set of constrained six degree-of-freedom parts, by working on a computer graphics analogy of the system. The system of equations are then assembled into matrix form and solved through time. The simulation results are interrogated using computer animations and data graphs.

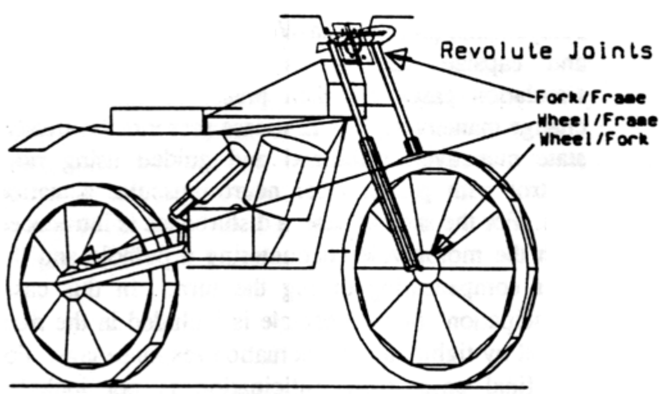

Fig. 2 The Motorcycle Model.

The motorcycle model used in this investigation is a lightweight "dirtbike" version. The principal physical characteristics are:

Weight:	100 kg
Wheelbase:	1325 mm
Tires:	110 mm x 350 mm (front)
	110 mm x 300 mm (rear)

The model consists of 4 parts, each with 6 degrees-of-freedom. In this model, the frame and engine assembly are to be considered one part and the fork and the two wheels are the other three. Degrees-of freedom are removed from the system using joints. The fork is connected to the frame via a hinge or revolute joint. Revolute joints also connect the tires to the frame. The effects of the suspension system are not included in this inquiry.

The wheels on the motorcycle are spinning parts with inertia properties, that generate the proper gyroscopic forces which dampen the motorcycle roll mode. The interaction between the road and the motorcycle is calculated using ADAMS/Tire™. ADAMS/Tire is a modular system of differential equations used to generate the longitudinal ground-tire reaction forces and lateral sliding forces, as well as the torques which result from conditions at the tire-road surface contact patch. These forces and torques are calculated at the contact patch and transferred to the spindle location automatically at each simulation time step.

For the 3 simulations detailed in this inquiry, the motorcycle is driven using a constant velocity kinematic driver on the rear wheel revolute joint. The speed through the lane change is 30.0 mph.

The system of equations built by ADAMS for the motorcycle model, results in 8 degrees-of-freedom including yaw, pitch, roll, lateral, longitudinal, vertical freedoms for the gross vehicle, and the rotational freedoms for the front wheel and the fork assembly. The rear wheel has 0 degrees-of-freedom with the addition of the kinematic driver. The principal modes of interest in motorcycle lateral-directional dynamics include a:

* <u>Capsize mode</u> relating to vehicle roll. This mode may gradually diverge in the absence of rider control.

* <u>Weave mode</u> involving the coupled roll and yaw motions of the motorcycle. This mode is always present even under rider control.

* <u>Wobble mode</u> (flutter mode) involving a response of the front fork assembly about its hinge point. This mode is always present even under rider control.

THE HUMAN SURROGATE RIDER MODEL - The rider dynamics comprise the controller element of the rider/cycle system. The human surrogate rider model attached to the motorcycle, is a dynamic multi-segment model which is capable of affecting or controlling the motorcycle during the riding event (active mode), as well as responding anthropometrically during the crash event (passive mode). The active and passive modes are switchable during the simulation, depending on the current status of the rider/cycle model.

The human surrogate rider model is created using the

ADAMS/Android™ preprocessor [12]. The model consists of 15 body segments, with mass and inertia scaled to represent a 80th-percentile male. The mass properties as well as the lengths of the major and minor axes of the ellipsoids representing the body segments, are automatically generated using an implementation of GEBOD (Generation of Body Data) [13] in ADAMS/Android.

The active rider control mode is accomplished using a dynamic compensator, discussed subsequently. The compensator senses motorcycle roll, yaw and path deviation and actuates the human surrogate rider to adjust the steer torque input to stabilize the vehicle, and to adjust its lean angle to maintain the proper heading.

The passive crash response mode is accomplished using torques acting at the joints between the segments of the surrogate, to model the proper kinematic rebound during a free-fall impact. The torques are based on stiffness, damping and friction data measured at the Armstrong Aerospace Medical Research Laboratory, Wright Patterson Air Force Base [14] from the HYBRID III [15] crash dummy. The nonlinear stiffnesses are included for each degree-of-freedom for each joint in the form of look-up tables. These data can be typically represented by the curve form shown in figure 3. This curve describes a small (or non-existent) stiffness throughout the normal operating range for a particular joint at a particular degree of freedom. The sharp inclines and declines of the curve are a result of the joint encountering hard-tissue resistance, or exceeding the biological limit for both positive and negative rotations. It is within this range that injury can occur to the joint.

These torque data derived from the HYBRID III are generally considered a passive response model for kinematic rebound simulation, representing a human unaware of the impending collision. The torque slope is altered for the rider model, using a scale factor to represent the rider recognizing the pending crash and "freezing."

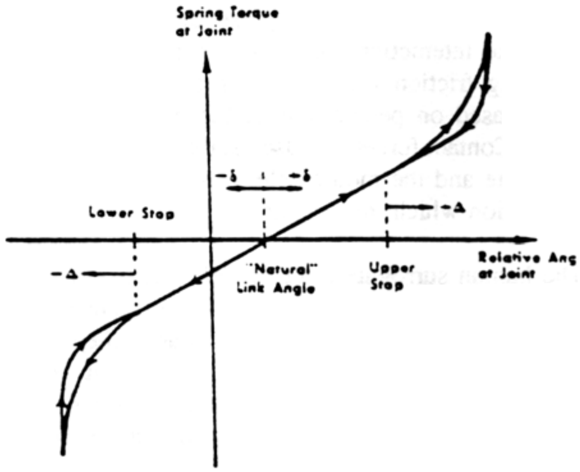

Fig. 3 Anthropometric Joint Torque Curve Form.

Once the surrogate model is physically specified, it is then manipulated into the riding position and connected to the motorcycle to form the combined rider/cycle system. The man/machine connections are implemented using break-away forces which release when the force is greater than a pre-established threshold. Connections are created for the lower arms to handle bars, feet to foot pegs and pelvis to seat. The break-away threshold for this investigation is the normal grasp strength of a 80th-percentile male for the arms to handle bars connection and slightly less for the other connections.

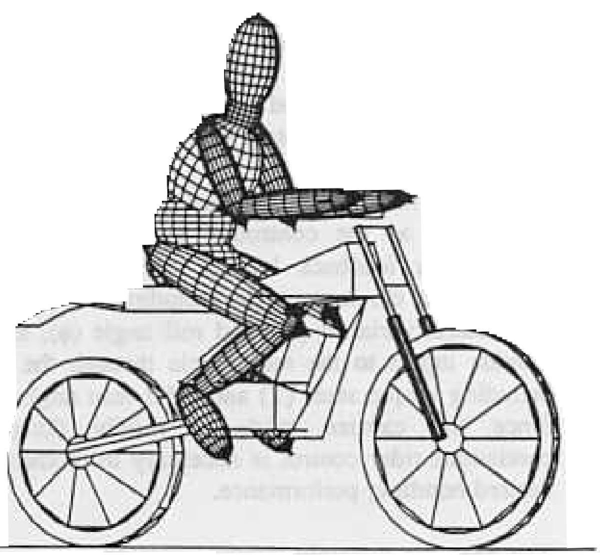

Fig. 4 The Combined Rider/Cycle Model.

Contact forces are established between all 15 body segments of the surrogate and ground to model the proper kinematic rebound of the surrogate during the crash. These contacts are represented using ellipsoid-flat plate interaction forces which generate motion-opposing friction forces when sliding and a normal force based on penetration of the ellipsoid into the plate. Contact forces are also established between the surrogate and the motorcycle to model any crushing interaction which may occur.

The human surrogate rider model switches from the active control mode to the passive response mode, when the break-away forces reach their force threshold and begin to detach. This limit will be exceeded, when the inertial forces of the rider caused by the crash are sufficient enough to remove the rider from the vehicle. It is assumed at this stage, that the rider will now be in a passive crash rebound mode and not in an active motorcycle control mode.

RIDER/CYCLE DYNAMIC COMPENSATOR - Given the elements that make up the combined rider/cycle model, ADAMS automatically generates the non-linear governing equations. These governing equations for the combined rider/cycle system are written in a surplus set of coordinates [16], resulting in a system of implicit first order differential-algebraic equations given as:

$$g(\underline{Y},\dot{\underline{Y}},t)=0 \qquad \text{Eq.1}$$

where $\underline{Y}$ = vector of system states
t = independent variable time

Because of this implicit formulation, system states may be directly coupled to other system states. For example, the lean-angle position of the rider may be a function of the desired maneuver, or heading and path variance of the motorcycle.

With the rider model as the controller and the motorcycle as the controlled system, a dynamic compensator feedback loop is necessary to sense output from the motorcycle including heading (ψ), path lateral variance (Δ), and roll angle (ϕ), and to provide inputs to the motorcycle through the rider including torque steer (T) and rider lean angle (ϕ_R). Since the capsize mode is mildly divergent, continuous rider control is necessary to produce the desired handling performance.

The example dynamic compensator chosen for this inquiry is the multiple loop, parallel structure type presented in Weir [6], and displayed in figure 5. It functions with an inner loop which serves to stabilize the roll of the vehicle (ϕ) using torque steer (T). This loop stabilizes the capsize mode and permits the path-related heading (ψ) and path lateral variance (Δ) loops to function.

An alternative series structure displayed in figure 6, feeds the rider lean input (ϕ_R) into the roll angle summer, providing only steer torque input (T) to the rider/cycle system.

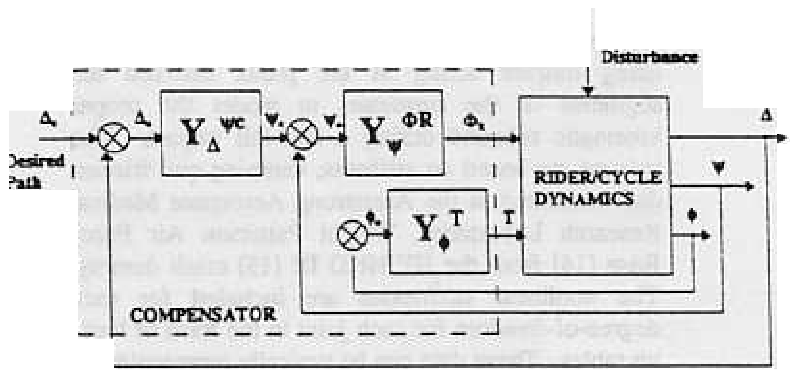

Fig. 5 Parallel Structure Rider Control System.

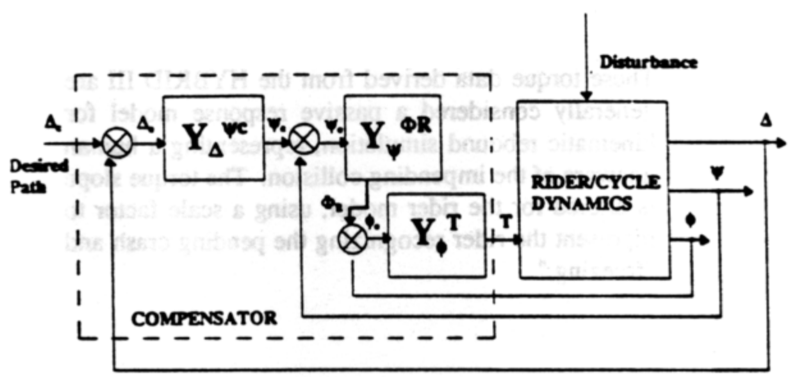

Fig. 6 Series Structure Rider Control System.

The parallel structure compensator was selected over the series structure for convenience, and since the mass ratio of the rider to the cycle is relatively high (85kg/100kg), and the speed relatively low (30 mph). With this condition, the lateral imbalance caused by rider lean will have an effect on the cycle dynamics [8]. This effect is included explicitly in the parallel structure compensator, but not in the series structure compensator.

In addition, the inclusion of rider lean in the control of a mechanical system serves to highlight a product distinction between ADAMS and general Crash Victim Simulation, CVS, programs. Currently, most of the existing CVS programs [17,18] are incapable of having the human surrogate model interact with and effect a mechanical environment in a feedback relationship. They are mostly used to provide a passive rebound response of the surrogate during a crash. The intent of this inquiry is to highlight both the <u>active</u> motorcycle controlling phase, and the <u>passive</u> crash response phase of ADAMS model for the human surrogate rider.

The parallel structure compensator is implemented in the ADAMS rider/cycle model in a stepwise fashion in the time domain. Procedures for implementing the compensator in the transformed domain or the state space domain are outlined in the appendix.

The inner loop is implemented and stabilized first. A simple gain ($-K_\phi^T$) is applied to the phase shifted cycle roll angle (ϕ_e) and used to apply a torque (T) to the handlebar assembly. The gain is negative which results in a torque to the right when the motorcycle is rolling left. A first order filter is applied to the current simulation motorcycle roll angle to introduce a lag in the response.

$$\tau\dot{\phi}_e+\phi_e=\phi_c \qquad \text{Eq. 2}$$

This equation phase shifts the roll angle (ϕ_e) through the use of the current cycle roll angle (ϕ) and a time lag constant (τ). This time delay effect is included to model the human actuation delay inherent in the neuro-muscular system dynamics. In the case of the arm-hand actuation of the handlebar, this amounts to a time delay (τ) of about .1-.3 seconds for an attentive rider [6].

A value for the gain ($-K_\phi^T$) is derived empirically. ADAMS/Linear™ is used to generate a linearized representation of the ADAMS model. Stability properties are observed by examining the Eigenvalues for the capsize mode of the system disturbed with a lateral intermittent force. The gain value ($-K_\phi^T$) for the rider/cycle model is determined, iteratively, to be $-6.578e^3$ N-mm/rad. With this gain, the nominal cycle roll angles are corrected in a rapid, well damped manner and the system stabilizes when influenced by a lateral disturbance.

With the inner stabilizing loop operating, the gains for path error to heading ($K_\Delta^{\psi c}$) and the heading error to rider lean angle ($K_\psi^{\phi R}$) are determined using the same empirical method. This time, the Eigenvalues for the capsize, wobble and weave modes are examined to determine system stability. This results in a path error to heading gain ($K_\Delta^{\psi c}$) of $3.373e^{-6}$ rad/mm and a heading to lean angle gain ($K_\psi^{\phi R}$) of 2.67 rad/rad.

The rider model responds to the lean angle signal from the compensator (ϕ_R) by rotating at the lumbar joint. The steer torque input (T) is applied directly to the fork assembly and not by actuating the rider's arms and hands. This will result in decreased damping in the wobble mode. This simplification is used to avoid the complexity of generating another control system, which decouples the physical leaning action from the steering action of the human surrogate.

SIMULATIONS

CASE 1: THE STABILIZED LANE CHANGE MANEUVER WITHOUT ROAD POTHOLE - To create a baseline simulation, the lane change maneuver is performed for the steady state condition without a disturbance. Figure 7 displays the geometry of the lane change maneuver. The desired path which the path lateral variance (Δ) is input using a cubic spline. Out-tracking is enforced by injecting an initial open-loop, feedforward command, in the initial quarter second of simulation, to introduce a negative steer torque,

The closed-loop model is simulated for a duration of 3 seconds, with 300 data points.

Fig. 7 Geometry of the Lane Change Maneuver.

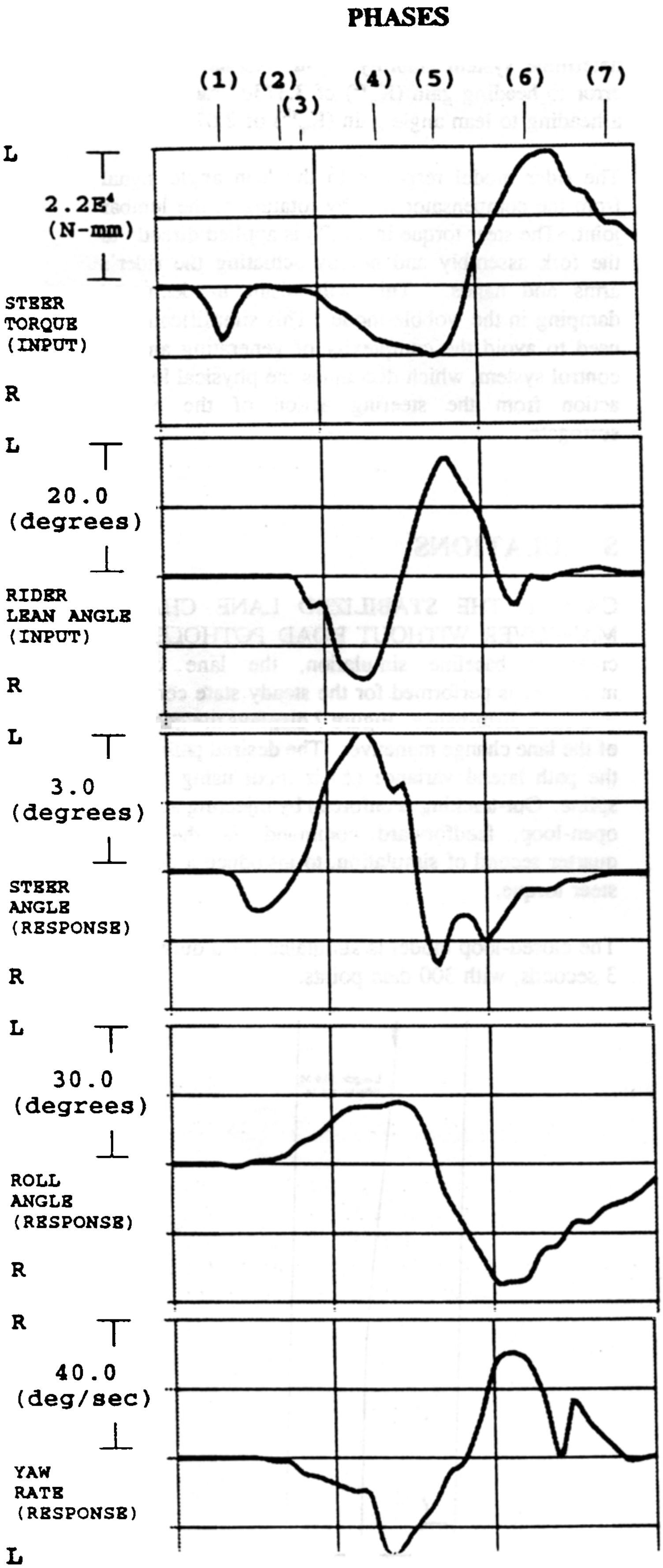

Fig. 8 Steady State Lane Change Maneuver.

Rider Control Response Analysis

One approach to obtaining an understanding of the rider/cycle system behavior is to examine the time histories of the control input and the motion responses of the system. The behavior of the rider/cycle system for this initial steady-state case is detailed in time history graphs in figure 8.

Stage (1) The maneuver is initiated by the open-loop application of steering torque to the right, causing small out-tracking steer angle to the right to develop.

Stage (2) With this forced torque input, the cycle begins to roll to the left and yaw to the left.

Stage (3) Within the .3 second time delay of sensing the path deviation due to the out-tracking, the rider begins to lean to the right, this causes the cycle to accelerate the roll rate to the left and the steer angle also goes to the left. With this shift in steer angle, the compensating steer torque also changes sign.

Stage (4) Peak cornering to the left occurs (roll angle and yaw rate are at maximum values).

Stage (5) The path error becomes large as the right turn phase occurs, causing the rider to lean to the left.

Stage (6) This causes the cycle to roll to the right and change sign in the steer angle. A large amount of steer torque is used to compensate for the lean to the left during this right cornering portion.

Stage (7) The maneuver is completed, with some path overshoot. The steer torque and rider lean inputs approach zero.

CASE 2: THE STABILIZED LANE CHANGE MANEUVER WITH POTHOLE DISTURBANCE - The lane change maneuver is now performed for the disturbance case. The location of the pothole will be at the peak of the left turn in the maneuver. The pothole is introduced into the simulation, by changing the road geometry from a continuous flat surface to a flat surface with a stepped variance. The pothole depth is 50 mm.

The pothole exists at the point when the motorcycle is at maximum roll, which causes an out-of-plane force to the front tire, and subsequently a lateral disturbance to the rider/cycle system. The effects of the control input (steer torque) and the motion response (cycle roll) for the stabilizing action are displayed in figure 9. The curves are overlayed on the curves of case 1 to highlight the effects caused by the disturbance on the steady-state condition.

In this figure, the disturbance to the roll motion is evident. The torque curve displays the corrective action taken by the compensator with the excited wobble mode superimposed. The .3 second time lag inherent in the rider neuro-muscular system can be observed by comparing the roll curve to the torque curve. Although the wobble mode is not damped, the roll disturbance is stabilized in a well damped manner.

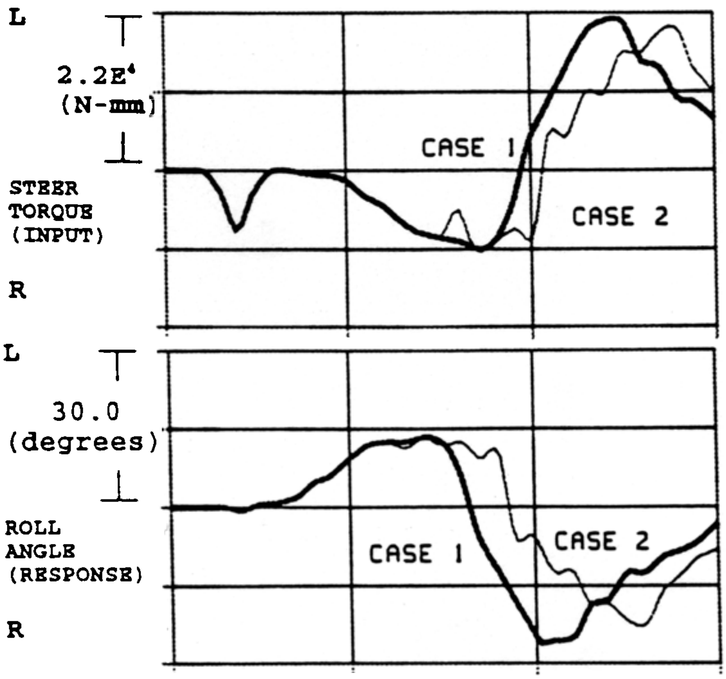

Fig.9 Stabilized Maneuver with Pothole Disturbance.

CASE 3: THE DE-STABILIZED LANE CHANGE MANEUVER WITH POTHOLE DISTURBANCE - Case 3 is put forth to investigate the possibility of rider inattentiveness as a source of error resulting in an instability and an injury producing crash. To model this inattentiveness, the time constant of equation (1), (τ) is modified from .3 to .4 seconds. This will have the effect of changing the response rate of the rider. Figure 10 displays the curves of case 3 overlayed on the curves of case 1.

In this figure, the added delay to the reaction time of the steer torque compensation is evident. The roll continues until the vehicle comes to rest on the pavement. The torque curve builds in oscillation and immediately goes to zero, indicating the rider model switching from the active, cycle control mode to the passive collision response mode.

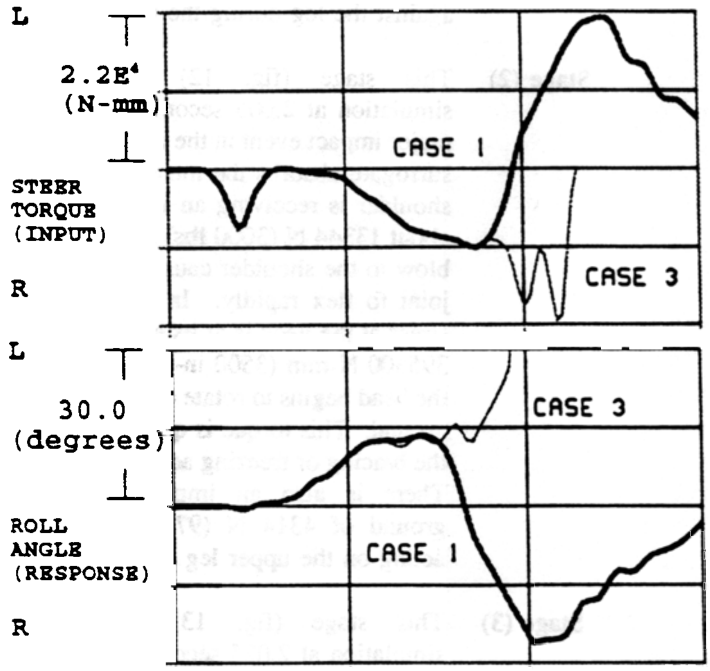

Fig. 10 De-Stabilized Maneuver with Pothole Disturbance.

Biodynamic Rebound Analysis

The next series of figures illustrates the resulting crash event for case 3. It is apparent from the kinematic rebound sequence that the rider does not react to the impending crash with any defensive posturing. For the purposes of this inquiry, it is assumed that the event occurs over such a short duration, .76 seconds, that the only posturing that the rider has time for is to "freeze." This effect is accounted for in the model by ramping up the stiffness coefficients in the HYBRID III anthropometric joint torque model.

Stage (1) This stage (fig. 11) displays the simulation at 1.945 seconds. This is the instant when the initial contact with ground occurs. It is at this time that the break-away forces which attach the feet and hands release. It can be observed from this figure that the foot is no longer positioned on the foot peg. At this time, the foot experiences a force from both the road (fig. 17) and the motorcycle (fig. 19) of about 800 N (180 lbs). This indicates that the foot as well as the foot peg, tires and handle bars are taking the load of the motorcycle impacting on the road. The leg receives loading previous to stage 1 (fig. 19), due to the motorcycle falling against the leg during the turn.

Stage (2) This stage (fig. 12) displays the simulation at 2.005 seconds. This is the major impact event in the crash, when the surrogate absorbs the most energy. The shoulder is receiving an impact force of about 13344 N (3000 lbs) (fig. 18). This blow to the shoulder causes the shoulder joint to flex rapidly. In this stage, the stress at the neck is at its highest point at 395500 N-mm (3500 in-lbs) (fig. 21), as the head begins to rotate down toward the ground. This torque is quite large due to the bracing or freezing action of the rider. There is also an impact force from ground of 4314 N (970 lbs) (fig. 17) acting on the upper leg of the rider.

Stage (3) This stage (fig. 13) displays the simulation at 2.025 seconds. This is the point when the head impacts the ground and the shoulder joint is at the highest torque level. The head impacts the ground and receives a force of 6672 N (1500 lbs) (fig. 17). This load is significantly reduced by the initial impact of the shoulder with the road and the high torque generated at the neck joint of 395500 N-mm (3500 in-lbs) (fig. 21) breaking the fall. Also in this stage, the large rotation of the shoulder joint can be seen resulting in a joint torque of 1356000 N-mm (12,000 in-lbs) (fig. 21).

Stage (4) This stage (fig. 14) displays the simulation at 2.205 seconds. In this stage, the rider is completely airborne after the rebound from the initial contact with the road. The right arm is displaced due to the friction of the road surface during the impact. Also, the body is rotating due to the frictional effects of the interaction between the right side of the body and ground. Since there is no contact with the ground at this time, there is no impact loading on the surrogate. There is relatively minor loading on the joints, with the largest on the lumbar spine at 22600 N-mm (200 in-lbs) (fig. 21).

Stage (5) This stage (fig. 15) displays the simulation at 2.3 seconds. In this stage, the rider begins to experience a second impact with ground. There is a foot impact of 356 N (80 lbs) between the road (fig. 17) and the motorcycle (fig. 19), indicating that the foot may be trapped underneath the motorcycle.

Stage (6) This stage (fig. 16) displays the simulation at 2.56 seconds. This represents the final position of the surrogate at the end of the simulation period. The forces and torques at this point are at a minimum.

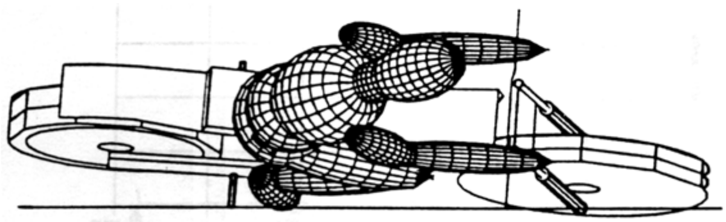

Fig. 11 Stage 1, Initial Impact (T=1.945).

SIDE VIEW

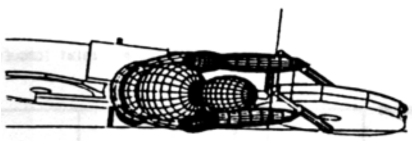

FRONT VIEW

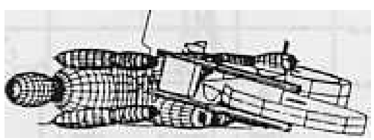

Fig. 12 Stage 2, Shoulder Impact (T=2.005).

SIDE VIEW

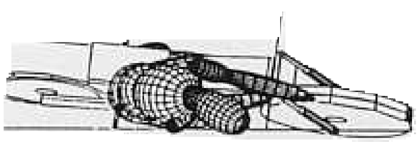

FRONT VIEW

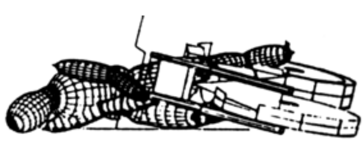

Fig. 13 Stage 3, Head Impact (T=2.025).

SIDE VIEW

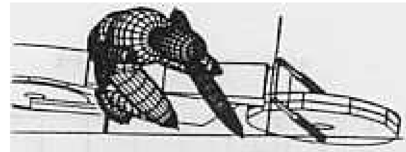

FRONT VIEW

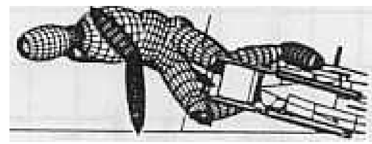

Fig. 14 Stage 4, Torso Twisting (T=2.205).

SIDE VIEW

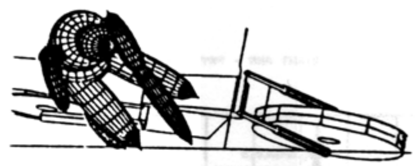

FRONT VIEW

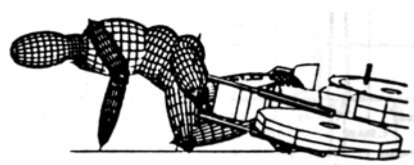

Fig. 15 Stage 5, Highest Bounce (T=2.3).

SIDE VIEW

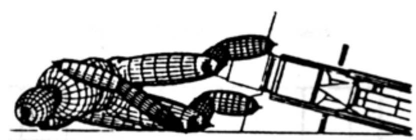

FRONT VIEW

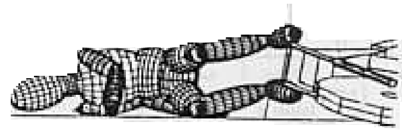

Fig. 16 Stage 6, Final Position (T=2.56).

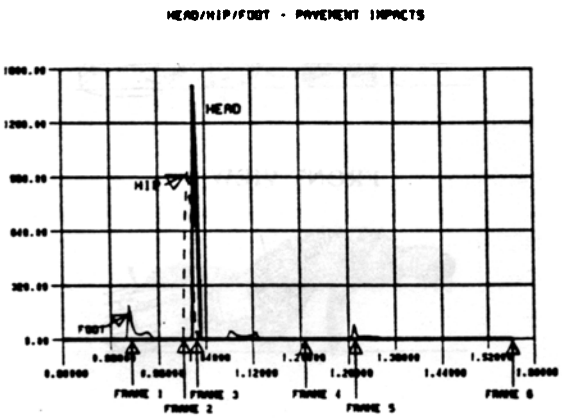

Fig. 17 Pavement Impacts (Head, Hip, Foot).

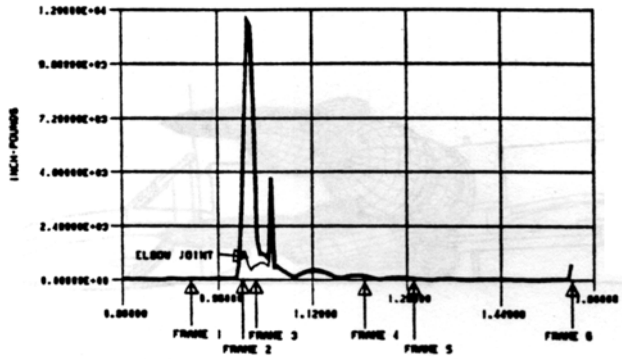

Fig. 20 Joint Torques (Arm).

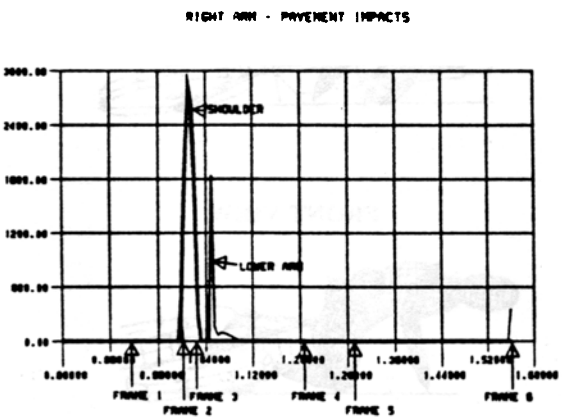

Fig. 18 Pavement Impacts (Arm).

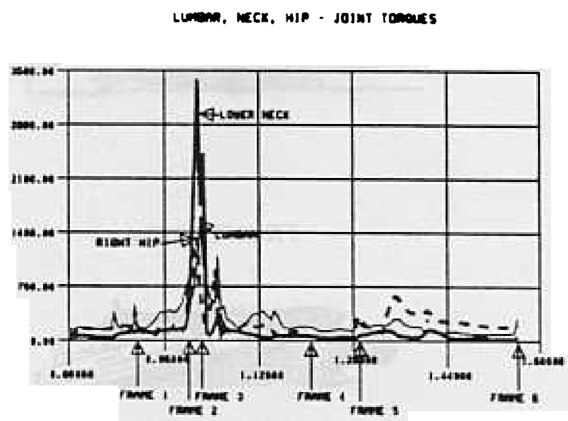

Fig. 21 Joint Torques (Lumbar, Neck, Hip).

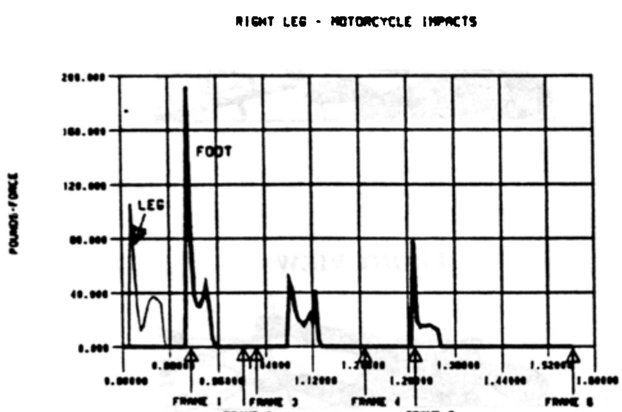

Fig. 19 Motorcycle Impacts (Leg).

Injury Analysis

Major injuries resulting from a vehicle crash, are generated by a change in velocity. That change in velocity may occur on a localized part of the body as a result of a specific blow, or it may be a whole-body velocity change. The actual response of the human frame, depends not only on the overall velocity change but on the varying accelerations which may occur during the impact phase. In addition, the external loading produces a biological response, which causes various relative motions and reactions to develop inside the human body. It is that human response which is, in essence, the biodynamics of trauma.

To determine if the human surrogate model is experiencing trauma during the simulated crash, the resulting forces and reactions must be recorded and compared against established injury tolerance criteria. Much data are available for head injuries, [19, 20, 21] including skull fracture data due to blows and brain injury data due to the forces resulting from translational and rotational acceleration. There are also data [19, 20, 22] for neck injury tolerance.

For the crash event simulated in this paper, the rider absorbs the majority of the crash energy during stage 2 (fig. 12). In this stage, the surrogate experiences an impact force of 13344 N (3000 lbs) which causes the shoulder joint to rotate and induce a torque of 1356000 N-mm (12,000 in-lbs). This loading causes the joint to exceed its biological limit and causes extreme strain. The joint torque of 1356000 N-mm (12000 in-lbs) is more than enough load to cause injury [19].

Also in stage 2, the neck receives a torque of 384200 N-mm (3400 in-lbs), which is far above the volunteer pain threshold of 88140 N-mm (780 in-lbs) [19] and is likely to cause soft tissue damage.

In stage 3 (fig. 13), the head impacts the ground and is subjected to a force of 6227 N (1400 lbs) This is beyond the limit to cause skull fracture [20]. If the rider were wearing a helmet during the crash, the possibility of skull fracture would be greatly reduced, however, the torque on the neck would increase due to the added mass.

As illustrated by this crash simulation, the injury potential for this crash occurring at 30 miles per hour on a concrete surface is quite high. Based on the results from this simulation, there is a distinct probability of a skull fracture, a neck ligament injury and a shoulder injury. The probabilities of hip and foot injuries due to impact are somewhat less. Injuries caused by abrasions are not considered in this inquiry.

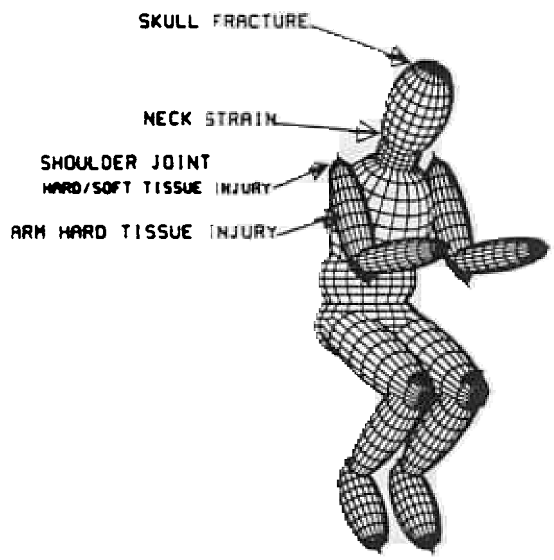

Fig. 22 High Probability Injury Zones to Rider.

CONCLUDING REMARKS

The intent of this paper is to provide a method of evaluating a motorcycle crash, both from the standpoint of rider/cycle control phenomenon as the source of the crash, and the interpretation of the injury producing mechanisms present during the crash. This paper has implications for motorcycle dynamics, rider control techniques, obstacle avoidance training, vehicle stabilization, motorcycle design and reliability analysis.

ACKNOWLEDGEMENT

The author would like to acknowledge with gratitude, the invaluable technical review provided by David Weir.

REFERENCES

1. Sharp, R.S. "The Stability and Control of Motorcycles." *Journal of Mechanical Engineering Science*, Vol. 13, No. 5, 1971.

2. Sharp, R.S. "The Influence of Frame Flexibility on the Lateral Stability of Motorcycles." *Journal of Mechanical Engineering Science*, Vol. 15, No. 2, 1975.

3. Sharp, R.S. "Dynamics of Single Track Vehicles." *Vehicle System Dynamics*, Vol. 4, No. 2-3, 1975.

4. Weir, D.H. "Motorcycle Handling Dynamics and Rider Control and the Effect of Design Configuration on Response and Performance." University of California at Los Angeles, Ph.D. Thesis, June 1972.

5. Weir, D.H. "A Manual Control View of Motorcycle Handling." Paper 73018, *Second International Congress of Automotive Safety*, San Francisco, July, 1973.

6. Weir, D.H. Zellner, J.W., "Lateral-Directional Motorcycle Dynamics and Rider Control", Paper 780304, *SAE Congress and Exposition*, Cobo Hall, Detroit, Michigan, February, 1978.

7. Eaton, D.J., "Man-Machine Dynamics in the Stabilization of Single-Track Vehicles." University of Michigan, Ph.D. Thesis, 1973.

8. Rice, R.S., "Rider Skill Influences on Motorcycle Maneuvering." Paper 780312, *SAE Congress and Exposition*, Cobo Hall, Detroit, Michigan, February, 1978.

9. Zellner, J.W., Weir, D.H., "Development of Handling Test Procedures for Motorcycles." Paper 780313, *SAE Congress and Exposition*, Cobo Hall, Detroit, Michigan, February, 1978.

10. Roland, R.D., "Computer Simulation of Bicycle Dynamics." *Mechanics and Sport, American Society of Mechanical Engineers*, 1973

11. ADAMS User's Manual, Mechanical Dynamics, Inc. Ann Arbor, MI., November 1991.

12. ADAMS/Android User's Manual, Mechanical Dynamics, Inc. Ann Arbor, MI., November 1991.

13. Baughman, L.D. "Development of an Interactive Computer Program to Produce Body Description Data" Dayton University, Ohio Research Institute, Contract no. F33615-81-6-0513, 1983.

14. Kelps, I.; et al. "Measurement of HYBRID III Dummy Properties and Analytical Simulation Data Base Development", Armstrong Aerospace Medical Research Laboratory Report no. AAMRL-TR-88-005.

15. Foster, J.K.; et al. "HYBRID III - A Biomechanically Based Crash Test Dummy", *Proceedings of the 21st Stapp Car Crash Conference*, 1977.

16. Chace, M.A., "Methods and Experience in Computer Aided Design of Large-Displacement Mechanical Systems", *Computer Aided Analysis and Optimization of Mechanical Systems*, NATO ASI Series F, Vol. 9, Springer-Verlag, Heidelberg, 1984.

17. MADYMO 3D User's Manual, TNO, the Hague, the Netherlands, April, 1990.

18. ATB User's Manual, AAMRL-TR-88-043, Wright Patterson Airforce Base, January, 1988.

19. Society of Automotive Engineers, "Human Tolerance to Impact Conditions as Related to Motor Vehicle Design", SAE Information Report no. J885, 1986.

20. Ommaya, A. K.; and Goldsmith, W. "Head and Neck Injury Criteria and Tolerance Levels", *The Biomechanics of Impact Trauma*. Elsevier Science Publishers B.V., Amsterdam, 1984.

21. Thibault, L.E.; Gennarelli, T.A. "Brain Injury: An Analysis of Neural and Neurovascular Trauma in the Nonhuman Primate", *Association for the Advancement of Automotive Medicine Conference Proceedings*, Scottsdale, Arizona, 1990.

22. McKenzie, J.A.; Williams, J.F. "The Dynamic Behavior of the Head and Cervical Spine During Whiplash", *Journal of Biomechanics*, Vol. 4, 1971.

23. Friedland, B., Control Systems Design: *An Introduction to State-Space Methods*, McGraw-Hill Book Company, 1986.

24. MATRIX_X User's Guide, Integrated Systems, Inc., Santa Clara, CA., January 1990.

25. Bryson Jr., A.E., "New Concepts in Control Theory, 1959-1984", Paper 84-0161. Presented at the *AIAA 22nd Aerospace Sciences Meeting*, Reno, Nev. 1984.

26. Sohoni, V.N., Whitesell, J., "Automatic Linearization of Constrained Dynamical Models", *ASME J. of Mechanisms, Transmissions and Automation in Design*, vol. 108, No. 3, pp. 300-304, September 1986.

MATRIXX is a registered trademark of Integrated Systems, Inc. (ISI).

ADAMS is a registered trademark of Mechanical Dynamics Inc. (MDI).

ADAMS/Android ADAMS/Tire and ADAMS/Linear are trademarks of MDI.

APPENDIX

GENERATION OF A RIDER CONTROL SYSTEM IN THE STATE SPACE DOMAIN - A dynamic compensator may also be developed and tuned in the state space domain [23]. To implement the series structure compensator of figure 6, the equations representing the rider/cycle system are linearized for export into controller design software such as $\text{MATRIX}_X^{\text{TM}}$ [24], where classic control design methodologies (root locus, Bode plots,...) or modern methods (pole placement, LQG,...) are available for control design [25]. When the compensator is designed, the equations representing this dynamic compensator are imported into ADAMS and combined with equation (1), coupling the various system states for the simulation of the complete closed loop system.

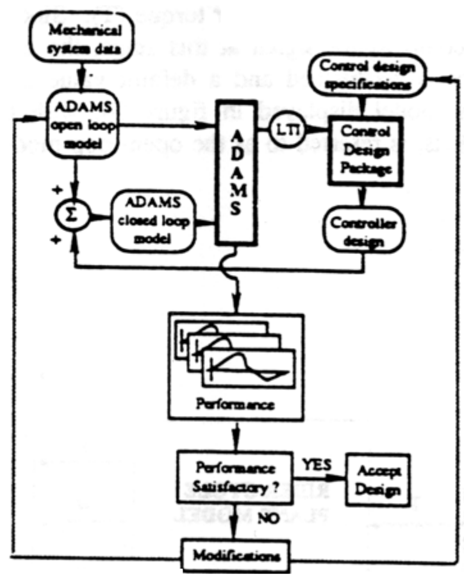

Fig. 23 Schematic of the General Compensator Design Methodology in State Space.

Figure 23 displays the general methodology for developing a dynamic controller in state space, and generating a simulation of a controlled closed-loop system. The steps involved in this methodology include:

1) Generate the non-linear, open-loop rider/cycle model and place it in the nominal position.

2) Linearize the equations of motion into a state space representation (plant model) of the open-loop system.

3) Import the plant model into $MATRIX_X$ and use control design methodologies to develop a dynamic compensator for the capsize stabilizing and the path following loops of for the series structure compensator of figure 6.

4) Export the compensator into ADAMS to perform the simulations on the closed-loop model.

First, an open-loop model for the system is defined by designating the inputs and outputs to the model and terminating the connections using special input/output "socket" elements. These socket elements will provide connection to the imported compensator. Figure 24 displays the open-loop model of the rider/cycle model. The outputs from the "plant" are the motorcycle heading (ψ), path lateral variance (Δ), and roll angle (ϕ). The input into the plant model is the correction signal from the compensator to the actuator to adjust the steer torque (T). Since there is no compensator signal at this stage, the connection point is established and a default value is entered. This model displayed in figure 24, with the open sockets, is referred to as the open-loop model.

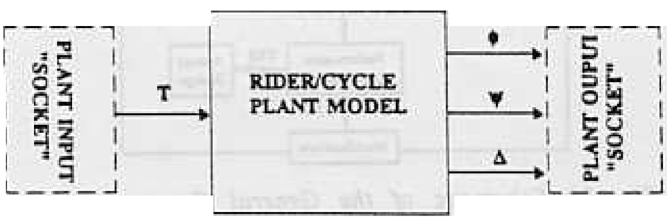

Fig. 24 The Open-Loop Model.

When the model is placed in the nominal position and the open-loop system established, the system of equations are linearized into a state space representation in the form of real valued state matrices ($\underline{A}$, $\underline{B}$, $\underline{C}$ and $\underline{D}$). Through the linearization process, the model as represented in equation (1) and by figure 24, is now represented as the linear state equations:

$$\dot{x} = \underline{A}x + \underline{B}u$$
$$\underline{y} = \underline{C}x + \underline{D}u \qquad \text{Eq. 3}$$

$\underline{x}$ represents the state variables for the plant model, $\underline{u}$ represents the inputs to the plant model, $\underline{y}$ represents the outputs from the plant model, and $\underline{A}$, $\underline{B}$, $\underline{C}$, and $\underline{D}$ are state matrices representing the plant.

ADAMS/Linear uses a condensation scheme to reduce a non-linear ADAMS model to a minimal realization linear form for efficient solution [26]. The state space model representation is suitable for obtaining frequency response of the ADAMS model, verifying model control properties (controllability and observability), and designing feedback controllers for ADAMS models.

The $\underline{A}$, $\underline{B}$, $\underline{C}$ and $\underline{D}$ matrices are written out in the specific format for import into $MATRIX_X$.

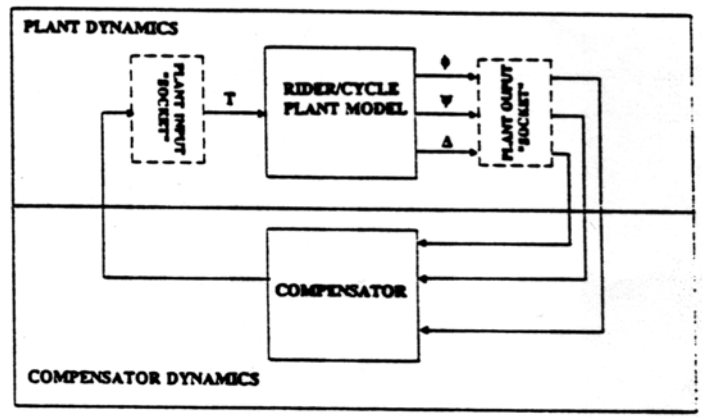

Fig. 25 The Closed-Loop Model.

After the compensator is developed and tuned in $MATRIX_X$, the $\underline{A}$, $\underline{B}$ and $\underline{C}$ matrices associated with the linear state equations representing the dynamic compensator are then exported from $MATRIX_X$ into ADAMS. When the compensator is read into ADAMS it is "plugged in" to the sockets of the plant model. The inputs to the compensator are connected to the plant outputs (ψ,Δ,ϕ). Also, output from the compensator is connected to the plant input (T).

With the addition of the compensator, and all connections established, ADAMS is then used to perform the simulations on the closed-loop model illustrated in figure 25.